■ 2389

A novel autonomous wireless sensor node for IoT applications

Ngan Nguyen, Quoc Cuong Nguyen, Minh Thuy Le*
School of Electrical Engineering, Hanoi University of Science and Technology, 10000, Vietnam
*Corresponding author, e-mail: thuy.leminh@hust.edu.vn

Abstract

A novel wireless sensor network node (WSNN) is presented in this paper where the solar energy harvester system is used as an autonomous power solution for endless battery lifetime. In this sensor node, the meander-line Inverted-F-Antenna (MIFA) is proposed and integrated in a single-CC2650 chip of Texas Instrument. The simple structure, low cost, compact size, high efficiency and low power consumption are advantages of this single-chip WSNN. The experimental results show that MIFA antenna is promising solution to enhance communication performance in WSN. In addition, the investigated single-chip WSNN with multi-wireless technologies including Bluetooth Low Energy and Zigbee as well as 6LowPAN is an attractive device for internet of thing (IoT) applications.

Keywords: 6LoWPAN, bluetooth, meander-line IFA (MIFA), wireless sennsor network node (WSNN), zigbee

1. Introduction

Wireless sensor network node is the most important member of Internet of Things (IoT) that enable to collect and exchange data with existing network and infrastructure [1-5]. WSNNs are often built with simple technique at affordable price, lightweight, low power consumption and compact size [6]. It must provide wireless network configuration with reliable and robust network connections and extend wireless connectivity range as far as possible. A simple node comprises of dozens of components: microcontroller, power supply, power management, sensor, memory, radio chip and antenna. Implementation of cost-effective miniaturized WSNNs requires high-level integration of various electronic modules.

A number of popular WSNNs have been reported in [7-11] such as Mica Z, Telos B, Tiny Node, Sun SPOT, Lotus these nodes are usually multi-chips, a node is built from one microcontroller and one RF transceiver module. Besides, traditional WSNN has the limitted lifetime of battery. Therefore, a periodic battery replacement is needed and the maintenant cost is required especially when the nodes are in complex positions. The disadvantages of these WSNNs are non-planar structure, high cost due to the RF transceiver module which used a MCU integrated RF profile and limited timelife. Nowadays, the system on chip (SOC) with built-in RF profile is a solution to design the low cost, compact size and high performance WSNN.

However, antenna integration solution is the big challenge of designing WSNN with built-in RF. This paper presents antenna solutions for a novel WSNN using CC2650 chip which supports multiple-wireless technologies including BLE, ZigBee, 6LoWPAN. An autonomous energy solution using solar energy harvester system is proposed in this WSNN design for endless battery lifetime. The proposed WSNN is also a solution for significantly saving cost, making the device compact, easily deployed, flexibility and scalability in wireless sensor networks for IoT.

The paper is organized as following: The proposed antenna integrated in wireless sensor network node is presented in section 2, autonomous wireless sensor network node using solar energy harvester system is shown in section 3 and wireless sensor network node experimention is expressed in section 4.

2. The Proposed Antenna Integrated in WSNN
2.1. Wireless Sensor Network Node Design

In the first step, the planar Inverted-F Antenna (IFA) antenna for WSNN is studied. This initial antenna consists of a thin arm or wire shorted at one of the ends to the ground plane [12-16], as shown in Figure 1 (a) is designed. The length of the arm is nearly $\lambda/4$. The input impedance is controlled by turning position of the feed. As the feed becomes closer to the shorting pin, the input impedance is reduced. Thus, to obtain a 50-ohm input impedance, the feed should be closer to the shorting pin than to the open end. The shorting pin introduces to the input impedance an inductance L_s while the open end introduces a capacitance Cs. To obtain the impedance at resonance frequency, the two reactive components should cancel out, leaving only the radiation resistance R_s. The width W of the shorting pin is very small compared to the wavelength ($W \ll \lambda$), usually $W \le (0.05-0.1)\,\lambda$.

As mentioned in the introduction, the WSNN must be small size and compact. It leads to miniaturize antenna dimensions for hardware design. In [17-20] several methods have been proposed for antenna miniaturization such as: folded antennas, lumped elements, using substrates with high dielectric constant, and multi-layer meta-material. With onboard antenna, the simplest structure is using a meander line or folded antenna. In [21], the simulated and evaluated meander line antenna geometry have studied. The idea is to fold the conductors back and forth to make the overall antenna shorter, it is a smaller area, but the radiation resistance, efficiency and bandwidth decrease. A meander-line antenna can be realized by bending the conventional IFA antenna to decrease the size of antenna. The influence of the meander part of the antenna is similar to a load and the meander line sections are considered as shorted-terminated transmission lines. The meander line sections can be modeled as an equivalent inductor. In the far-field pattern, the result of the cancellation of magnetic fields, the transmission lines of a meander line antenna do not radiate fields. The radiation fields will be radiated from the vertical pars of MIFA. After bending the arm of the IFA antenna (MIFA), we obtained the new antenna with much smaller size of 25% compared with the initial IFA antenna, the total antenna size is only 33.6*42.6 mm. The parameters dimensions of MIFA are shown in Table 1.
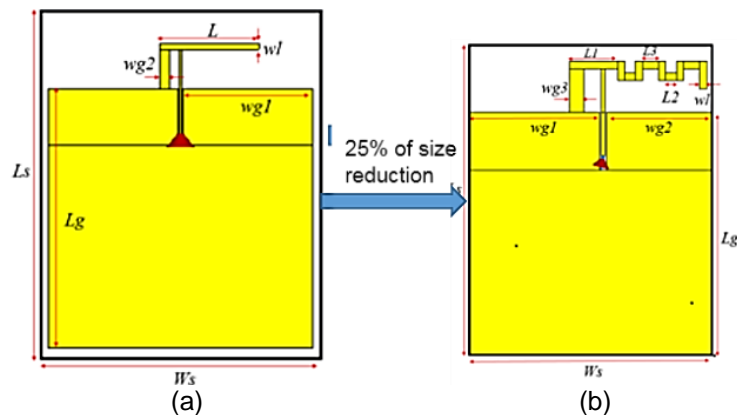

Figure 1. (a) The printed IFA (b) The meander line printed IFA (MIFA)

Table 1. Parameters Dimension of MIFA

Parameters	Value (mm)	Parameters	Value (mm)
L_g	34	W_{g1}	18.1
W_s	33.6	W_{g2}	14.56
L_s	42.6	W_{g3}	2
L_1	6.67	w_l	16
L_2	1.5	L_3	2.2

After completing the MIFA design, this antenna is integrated in WSNN, the reflection coefficient of the proposed MIFA in free space (the red line) and in the sensor node circuit (the black line) are presented in Figure 2. These results show that the resonant frequency is

shifted from 2.445 GHz to 2.5 GHz while the MIFA bandwidth is reduced 110 MHz when the MIFA is integrated into circuit. As shown in Figure 3, the novel single-chip WSNN uses only one chip SOC of CC2650. The CC2650 chip is a wireless MCU targeting Bluetooth, ZigBee and 6LoWPAN. This SOC chip is a member of the CC26xx family of cost-effective, ultralow power, 2.4 GHz RF devices. Very low active RF and MCU current and low-power mode current consumption provide excellent lifetime. The CC2650 device contains a 32-bit ARM Cortex-M3 processor that runs at 48 MHz as the main processor and a rich peripheral feature set that includes a unique ultralow power sensor controller. This sensor controller is ideal for interfacing external sensors and for collecting analog and digital data autonomously while the rest of the system is in sleep mode. Thus, the CC2650 device is ideal for WSN applications in a whole range of production including industrial, consumer electronics, and medical.
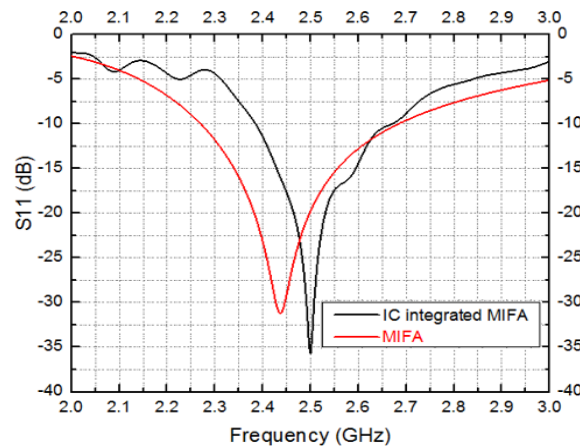

Figure 2. S11 coefficient of MIFA in free-space and model IC integrated MIFA

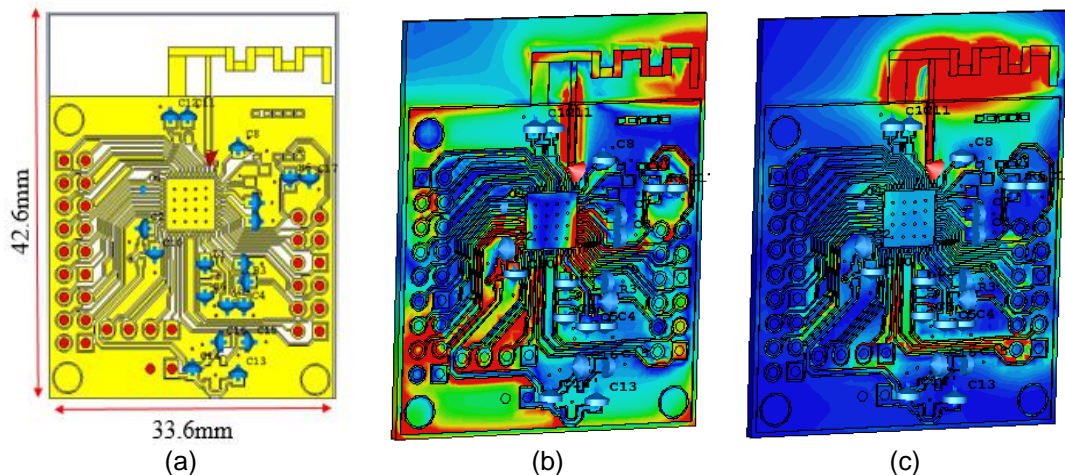| (a) | (b) | (c) |

Figure 3. (a) IC integrated MIFA model, (b) E-Field, (c) H-Field

Figure 4 shows 3D radiation pattern of IC integrated MIFA model with the peak gain of 1.74 dBi, total efficiency of 81%. A comparison between the proposed CC2650 WSNN and related work is shown in Table 2. It can be seen that this design achieves the compact size, simple structure, high performance and low cost, especially the power consumption of the WSNN is lower than some nodes in the market. The layout of proposed WSNN and the prototype is illustrated in Figure 5.
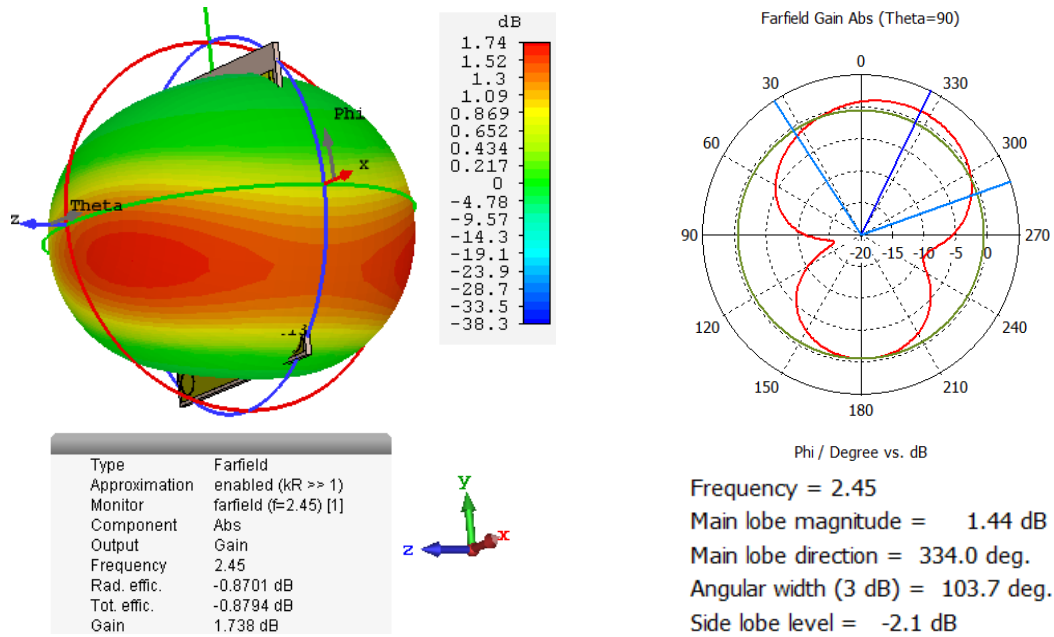
Type	Farfield
Approximation	enabled (kR >> 1)
Monitor	farfield (f=2.45) [1]
Component	Abs
Output	Gain
Frequency	2.45
Rad. effic.	-0.8701 dB
Tot. effic.	-0.8794 dB
Gain	1.738 dB

Frequency = 2.45
Main lobe magnitude =   1.44 dB
Main lobe direction = 334.0 deg.
Angular width (3 dB) = 103.7 deg.
Side lobe level =   -2.1 dB

Figure 4. The simulation of 3D radiation pattern and polar radiation pattern of
IC integrated MIFA model

(a)   (b)
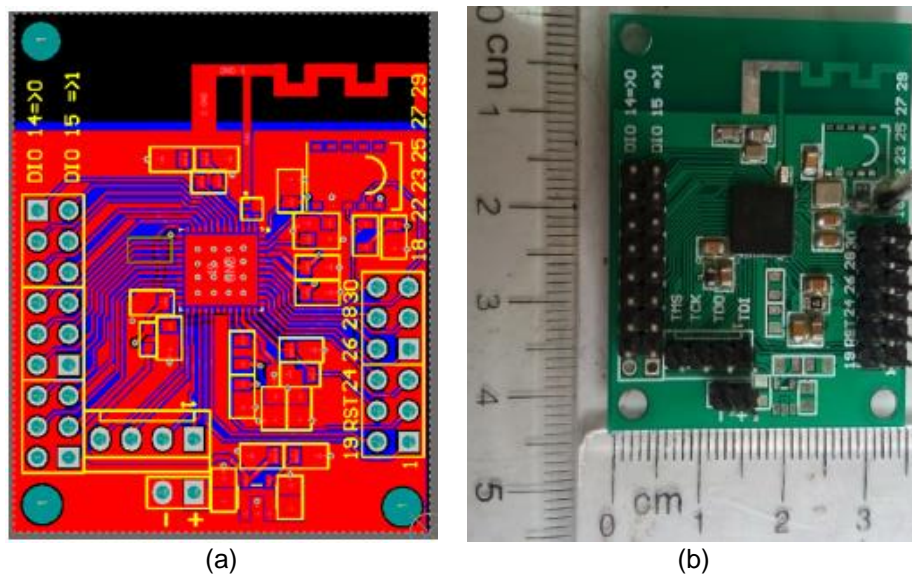
Figure 5. (a) PCB layout of CC2650 integrated MIFA (b) WSNN prototype

2.2. Antenna Gain Measurement

As the antenna is integrated in the sensor node circuit, the antenna gain measurement method is based on the Friis transmission formula, two sensor nodes are separated at a distance R of 4 m shown in Figure 6.
where:
- A wireless sensor node using an external antenna which actived as a peripheral for advertising using BLE communication technology, the transmit power P_t of this node is known. External antenna is omnidirectional dipole antenna with the peak gain of 2.01 dBi at 2.45 GHz.

- The CC2650 integrated MIFA actived as a central device which listening to the advertising data, the received power P_r of this node is known from the measured RSSI (Recevier Signal Strength Indicator) values. Texas Instrument has defined a rule to directly convert RSSI values into receive power P_r (dBm) [16].

Ideally, the losses due to impedance loss, impedance matching should be ignored and assumed that the transmitting and receiving antenna of WSNN are matched to their lines or loads, then Friss formula is reduced to [7].

$$G_r = \frac{P_r}{P_t} \cdot \left(\frac{4\pi R}{\lambda}\right)^2 \cdot \frac{1}{G_t} \quad (1)$$

Transmitting power of WSNN using external antenna is 0 dBm, then receiverd power measured by CC2650 WSNN is -60 dBm at the distance of 4 m. Therefore, the 0.087 dBi of measured gain of MIFA integrated WSNN is calculated by (1):

Figure 6. Gain measurement scenario of MIFA antenna integrated WSNN

2.3. Power Consumption Measurement

The power consumption measurement set up of the WSNN is presented in Figure 7 to calculate its lifetime. To measure current consumption in each operating mode of the device, using the oscilloscope to analyze the operation of the device in each mode is essential. Since the oscilloscope only has voltage transducers, a resistor connected in series with test equipment (DUT) is required. A 10 Ω resistor is an appropriate value so that it does not affect the circuit and can provide a voltage value that is large enough to be visible on the oscilloscope as shown in Figure 8. The power consumption is listed in Table 2.
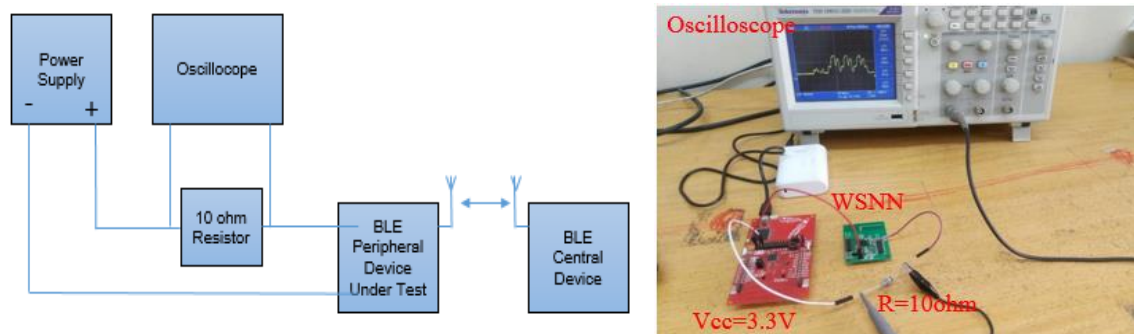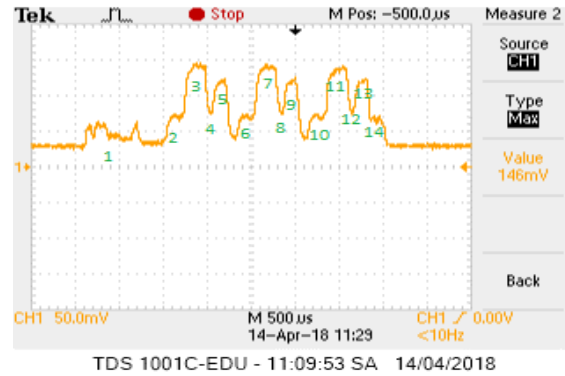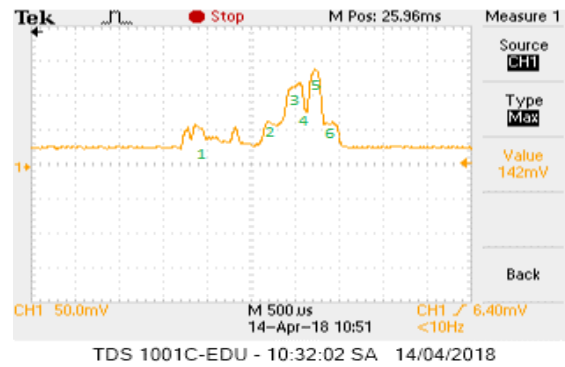

Figure 7. Power consumption measurement setup of the WSNN

(a)

(b)

Figure 8. Measurement results with BLE standard: (a) advertising mode (b) connecting mode

The power consumption of the WSNN is calculated as follows:

$$I = \frac{(t1 \; x \; I1) + (t2 \; x \; I2) + (t3 \; x \; I3) + ... + (t14 \; x \; I14)}{t1 + t2 + t3 + ... + t14} \tag{2}$$

with power supply of 3.3 V. We can calculate the device power in each mode as follows:

$$P = U * I \tag{3}$$

Table 2. Comparison of the Proposed CC2650 WSNN and Traditional WSNN

Ref.	WSNN	Size in (mm)	Cost	Wireless Technology	Power consumption	
					Active	Sleep
[22]	Mica Z	58*32	$99	ZigBee	91.4 mW	50 µW
[23]	Telos B	65*31	$99	IEEE 802.15.4	81.8 mW	25.5 µW
[24]	Lotus	76*34	$300	ZigBee	217.8 mW	33 µW
[25]	Iris	58*32	$115	ZigBee	79.2 mW	26.4 µW
This work	CC2650	33*42	$26	BLE	25.37 mW	0.33 µW
This work	CC2650	33*42	$26	6LowPan	50.66 mW	0.99 mW

3. Autonomous WSNN using Solar Energy Harvester System
3.1. Power Supply Based on Solar Energy Harvester System
The proposed sensor node is powered by a battery with the determined lifetime. A solar energy harvester system is added as in Figure 9 to obtain endless lifetime, this power supply solution makes wireless sensor node becomes an autonomous WSNN. In this article, the power supply includes a DC-DC converter circuit and energy storage. The problem is finding ways to manage the input voltage of the charger circuit. This leads to the idea of storing energy in the super capacitor before it is introduced into the charger circuit. Figure 10 presentes a voltage

monitor circuit that continuously monitors the stored voltage level and conducts a signal allowing the charging circuit to operate if it reaches a threshold. The function of this voltage monitor circuit is to control the operating time of the circuit and to ensure that solar panel always provides enough power to the circuit when the switch is enabled.

Storage blocks store energy at the desired voltage levels to use for different purposes. For energy storage, capacitors, supercapacitors or rechargeable batteries can be used. The selected components of this mission are PowerCast's IC PCC210, designed to raise the voltage effectively, allowing the desired voltage to be supplied to the load. Measured results at Figure 11 show that the output voltage of the solar charging circuit is stable at 3.4 V, enough to provide power for stable wireless sensor node operation.
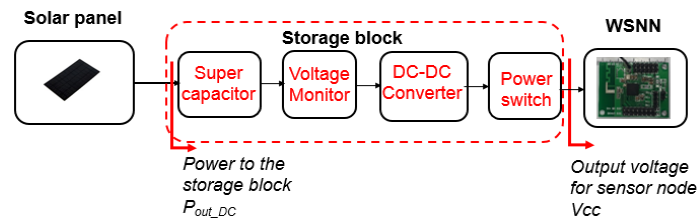

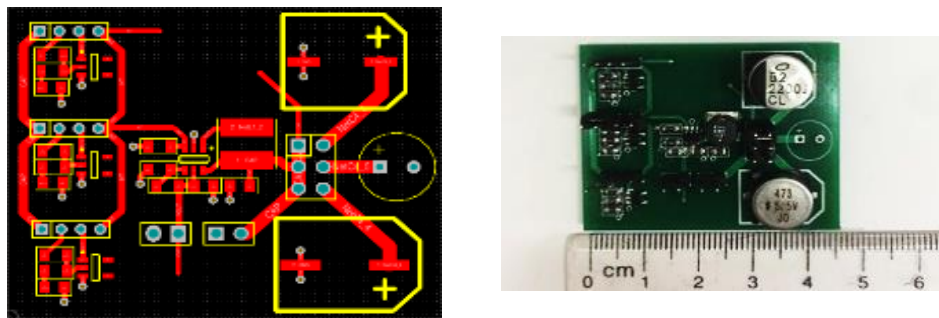Figure 9. Block diagram of solar energy harvesting system powering for the proposed WSNN

Figure 10. PCB design and prototype of voltage monitor circuit and energy storage
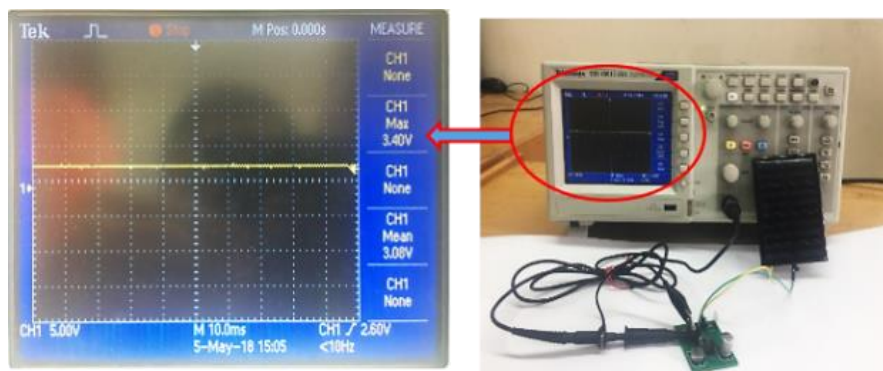

Figure 11. Power supply of WSNN using solar energy harvesting system

3.2. Wireless Sensor Node using Multi-wireless Technologies

WSNN supports three wireless communication technologies: Bluetooth Low Energy, 6LoWPAN, ZigBee. In this work, we conducted a test scenario to test the transceiver distance between two WSNNs using BLE technology with extremely low power consumption of only 25.37 mW in active mode. At the same time, we also built a wireless sensor network monitoring room temperature using 6LoWPAN technology with active mode power consumption of

50.66 mW. The process of data exchange between two BLE devices is described in Figure 12. The flowchart of the WSNN BLE and 6LoWPAN is presented in Figure 13.
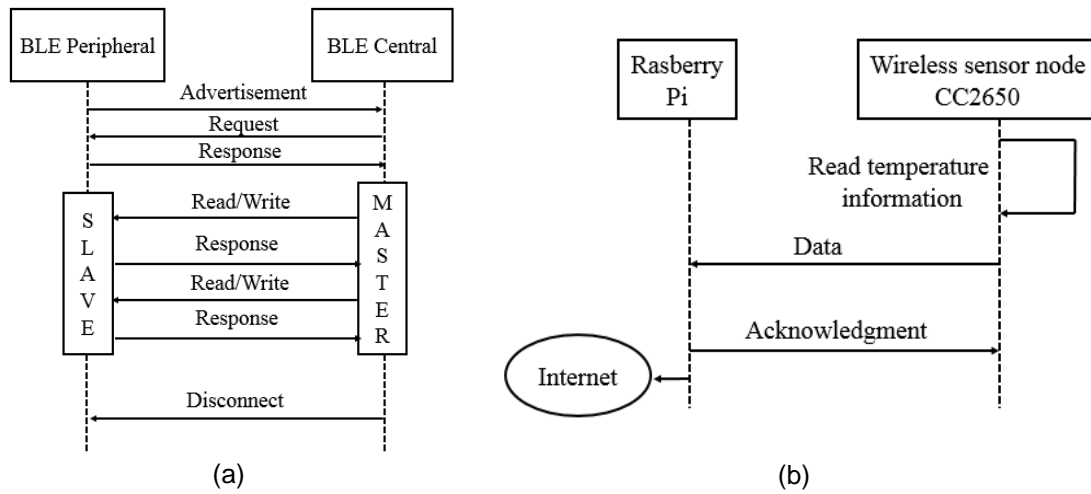

(a)   (b)

Figure 12. (a) The process of data exchange between two BLE devices
(b) The data flow between the WSNN and the Gateway program 6LoWPAN

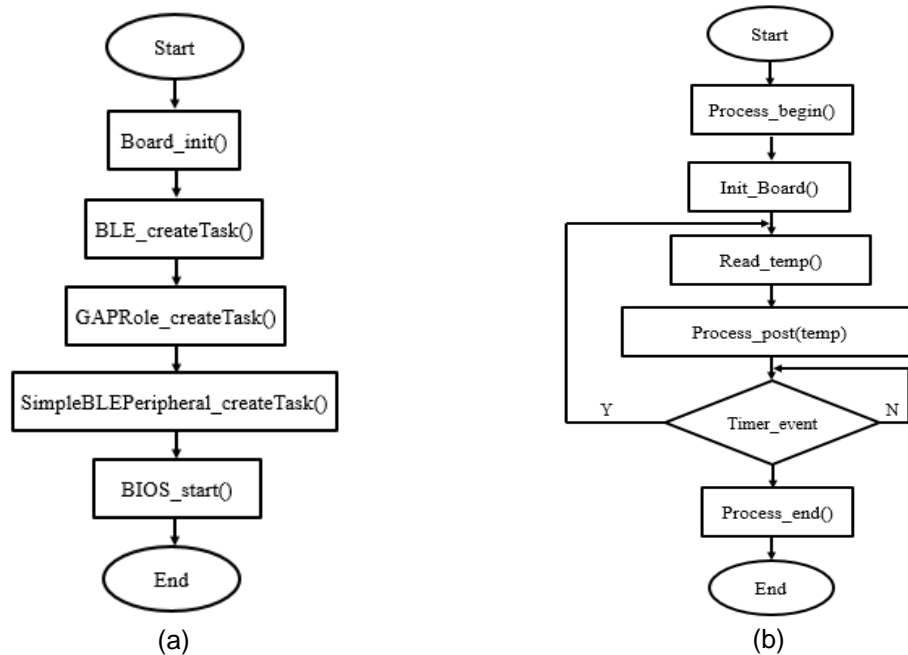(a)   (b)

Figure 13. (a) The flowchart of the WSNN BLE Peripheral program
(b) The flowchart of WSNN temperature reading program in 6LoWPAN network

4. WSNN Experimentation

In this simple scenario, the proposed WSNN is used in environment monitoring system showing its advantages in terms of computation, storage, time life and omni-directional communication. We conducted two scenarios with CC2650 WSNN: (1) read-range measurement between the two nodes using the Bluetooth Low Energy communication and; (2) an indoor temperature monitoring using wireless sensor network based on 6LoWPAN communication technology.

4.1. Scenario 1: Read-range Measurement

The distance of communication between two WSNNs using BLE communication standard is tested and measured in this experimentation as in Figure 14:
- Setting one WSNN in BLE Peripheral mode, one WSNN in BLE Central mode
- Setting the transmission power is 0dBm
- Transmitting 1000 packets between two nodes and calculating packet error rate (PER)
- Moving the WSNN to determine the antenna's multi-directional radiation
- The number of packets transmitted and received between the two sensing nodes will be monitored by the computer.

Table 3 illustrates the result of read-range measurement between two WSNNs using BLE communication standard. Two nodes can communicate together at a maximum distance of 64 m, the PER is 0.5%.
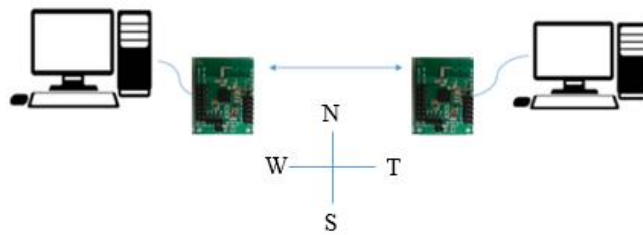

Figure 14 The measurement configuration of the read-range between
two WSNNs operating in BLE mode

Table 3. The Result of Read Range Measurement between Two WSNNs using BLE Technology

	WSNN integrated antenna	Direction of antenna	Distance between two WSNN				
			4 m	16 m	32 m	48 m	64 m
The number of packet received	MIFA	North	1000	1000	1000	1000	1000
	MIFA	South	1000	1000	999	1000	995
	MIFA	East	1000	1000	1000	1000	1000
	MIFA	West	1000	1000	1000	1000	999

4.1. Scenario 2: Indoor Temperature Monitoring using WSN based on 6LoWPAN technology

In the indoor temperature monitoring WNS as in Figure 15, the CC2650 WSNNs measure the temperature in a room and then transmit the measured date to the Raspberrypi3-Gateway. The CC2650 WSNNs send data to the gateway, from which the gateway sends data to the Internet via the MQTT protocol. Measuring cycle of each WSNN is set to 10 s for one measurement. The 6LoWPAN technology uses the IPv6 address of the device. In order to transport data from the wireless sensor node to the Internet, we need to use NAT64 to switch between IPv6 and IPv4. To do this, we used the software package provided by Wrapsix, installed the software package directly on the Rasberry Pi embedded computer. The temperature WSN prototopye is presented in Figure 16 with the website interface.
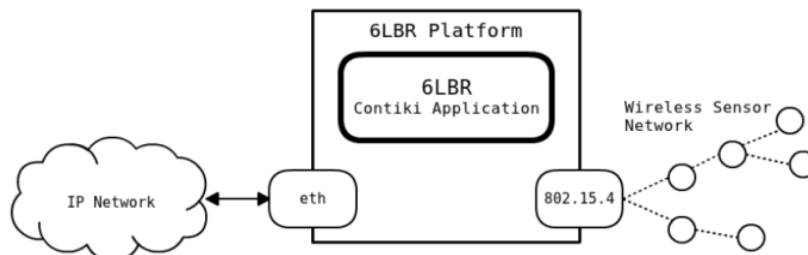

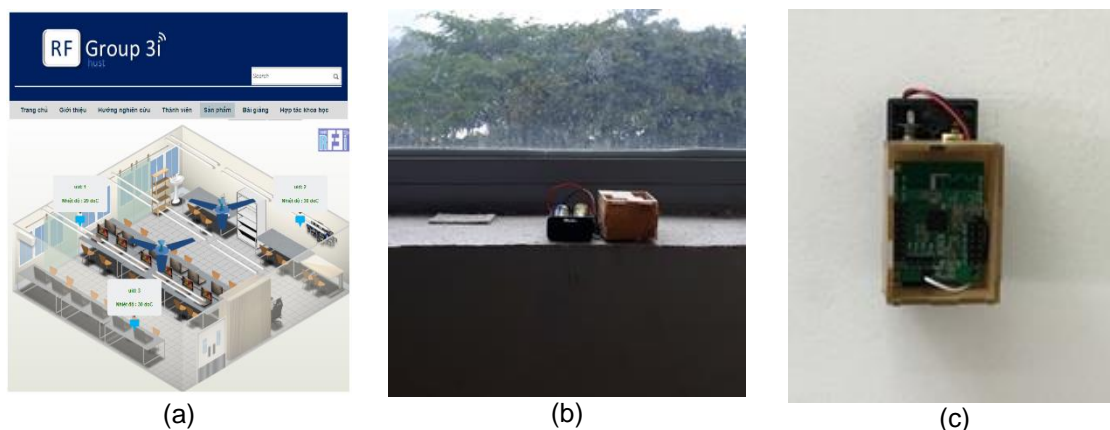Figure 15. System architecture for indoor temperature monitoring using WSN

Figure 16. (a) Website interface for indoor temperature monitoring;
(b) WSNN installed in the room; (c) Prototype

5. Conclusion

The proposed WSNN using MIFA antenna is working at the frequency band of Zigbee, Bluetooth low energy ad Wi-fi band. The simple structure and quasi-omnidirectional, compact size and low cost are advantages of this novel node. Besides, the planar structure, low power consumption and multi-wireless communication technologies allow this node to be an excellent wireless sensor network node in wireless sensor network and IoT applications. The WSNN is tested in a real scenario giving long read-range, very low power consumption and high PER. The limited battery lifetime challenge is solved using solar energy harvester system and store energy as well as voltage monitoring and battery charging. This solution helps WSNN to become an autonomous wireless sensor network node.

Acknowledgements

References

[1] SRJ Ramson, DJ Moni. *Applications of wireless sensor networks—A survey.* in 2017 International Conference on Innovations in Electrical. Electronics, Instrumentation and Media Technology (ICEEIMT). Coimbatore. 2017: 325–329.

[2] Y Liu. Wireless Sensor Network Applications in Smart Grid: Recent Trends and Challenges. *International Journal of Distributed Sensor Networks.* 2012; 8(9): 492819.

[3] MF Othman, K Shazali. Wireless Sensor Network Applications: A Study in Environment Monitoring System. *Procedia Engineering.* 2012; 41: 1204–1210.

[4] K Bi. Design and Implementation of the ZigBee Wireless Sensor Network Based on ARM. *International Journal of Online Engineering (iJOE).* 2017; 13(12): 76.

[5] M Erazo *et al. Design and implementation of a wireless sensor network for rose greenhouses monitoring.* in 2015 6th International Conference on Automation, Robotics and Applications (ICARA), Queenstown, New Zealand. 2015: 256–261.

[6] S Cheng. *Integrated antenna solutions for wireless sensor and millimeter-wave systems.* Uppsala: Acta Universitatis Upsaliensis. 2009.

[7] M Healy, T Newe, E. Lewis. Wireless Sensor Node hardware: A review. 2008: 621–624.

[8] N Pires, T Parra, AK Skrivervik, AA Moreira. Design and Measurement of a Differential Printed Antenna for a Wireless Sensor Network Node. *IEEE Antennas and Wireless Propagation Letters.* 2017; 16: 2228–2231.

[9] A Mainwaring *et al.* Wireless sensor networks for habitat monitoring. 2002: 88–97.

[10] K Piotrowski, P Langendoerfer, S Peter. *How public key cryptography influences wireless sensor node lifetime.* in Proceedings of the fourth ACM workshop on Security of ad hoc and sensor networks -SASN '06. Alexandria, Virginia, USA. 2006:169.

[11] M Maurya, SR Shukla. Current wireless sensor nodes (Motes): Performance metrics and constraints. *International Journal of Advanced Research in Electronics and Communication Engineering*. 2013; 2(1): 045.

[12] CA Balanis. *Antenna theory: analysis and design*, Fourth edition. Hoboken. NJ: Wiley. 2016.

[13] C Soras, M Karaboikis, G Tsachtsiris, V Makios. Analysis and design of an inverted-F antenna printed on a PCMCIA card for the 2.4 GHz ISM band. *IEEE Antennas and Propagation Magazine*. 2002; 44(1): 37–44.

[14] J-T Huang, J-H Shiao, J-M Wu. A Miniaturized Hilbert Inverted-F Antenna for Wireless Sensor Network Applications. *IEEE Transactions on Antennas and Propagation*. 2010; 58(9): 3100–3103.

[15] MZ Azad, M Ali. A Miniature Implanted Inverted-F Antenna for GPS Application. *IEEE Transactions on Antennas and Propagation*. 2009; 57(6): 1854–1858.

[16] M-C Huynh, W Stutzman. Ground plane effects on planar inverted-F antenna (PIFA) performance. *IEE Proceedings-Microwaves, Antennas and Propagation*. 2003; 150(4): 209.

[17] SS Holland. Miniaturization of microstrip patch antennas for GPS applications. 2008.

[18] R Kumar, JP Shinde, MD Uplane. Effect of slots in ground plane and patch on microstrip antenna performance. *International journal of recent trends in engineering*. 2009; 2(6): 34–36.

[19] M Fallahpour, R Zoughi. Antenna Miniaturization Techniques: A Review of Topology-and Material-Based Methods. *IEEE Antennas and Propagation Magazine*. 2018; 60(1): 38–50.

[20] D Upadhyay, RP Dwivedi. *Antenna miniaturization techniques for wireless applications.* in 2014 Eleventh International Conference on Wireless and Optical Communications Networks (WOCN), Vijayawada, Guntur District, Andhra Pradesh, India. 2014: 1–4.

[21] M Ma, K Deng. The study and implementation of meander line antenna for an integrated transceiver design. PhD Thesis, Master Thesis in Electronics/Telecommunications. 2010.

[22] Document online: micaz datasheet, http://www.memsic.com.

[23] Document online: telosb datasheet, http://www.memsic.com.

[24] Document online: Lotus datasheet, https://www.memsic.com.

[25] Document online: Iris datasheet, http://www.memsic.com.